Strong-Field Effects Driven by Mid-Infrared Light in Metal-Silicon-Metal Photodiodes

Tianyou Li, Omer Emre Ates, and William P. Putnam*
Department of Electrical and Computer Engineering,
University of California, Davis, 1 Shields Ave., Davis, CA 95616, USA
**Corresponding author: bputnam@ucdavis.edu*

Abstract: We illuminate nanoantenna-based, metal-silicon-metal photodetectors with ultrafast, mid-infrared laser pulses. We record the current versus pulse energy response and observe microamp-level currents, low effective nonlinearities, and strong-field signatures.
OCIS codes: (260.7120) Ultrafast phenomena; (250.5403) Plasmonics; (020.2649) Strong field laser physics

At high optical intensity, photoemission enters the strong-field regime. In this regime, photoemission resembles a tunneling process and enables intriguing effects such as low effective nonlinearities [1] and carrier-envelope-phase sensitivity [2]. Recently, strong-field photoemission from metallic nanostructures into vacuum has been intensively studied. However, a closely related process, strong-field internal photoemission has received comparatively little attention [3]. In internal photoemission, electrons are typically excited from a metal into an adjacent semiconductor. The mid-infrared portion of the electromagnetic spectrum offers an intriguing avenue to explore this process, as semiconductors can resemble transparent dielectrics to mid-infrared light. Additionally, there is currently a demand for novel, versatile mid-infrared detector technologies. Here, we explore strong-field effects in a metal-silicon-metal system driven by mid-infrared laser light. We illuminate arrays of nanotriangle antennas with ultrafast, mid-infrared laser pulses and observe current injection from the metallic antennas into the adjacent silicon.

Our experimental setup is shown in Fig. 1a. Arrays of gold nanotriangles are fabricated on a float-zone silicon substrate. As illustrated in Fig. 1a, the gold nanotriangles are illuminated by mid-infrared laser pulses. The infrared excitation drives electron emission from the nanotriangles, and emitted electrons drift from the nanotriangles (emitter) to adjacent wires (collector). A bias (V_B) is applied between the emitter and collector, and the current is measured. Electron micrographs of our devices are shown in Fig. 1b. The nanotriangle emitters and adjacent collectors have a thickness of 30 nm and rest on a 2-nm-thick Ti adhesion layer. The nanotriangles are interconnected by 200-nm-wide wires and are 300 nm from the nearby collectors. The devices are integrated in a 40 μm × 40 μm array of 140 devices. The spectrum of our mid-infrared excitation is shown in Fig. 1c. Our mid-infrared source is based on intra-pulse difference-frequency generation (IDFG) in a $ZnGeP_2$ (ZGP) crystal pumped by an amplified 2.4-µm, Cr-doped ZnSe/S mode-locked laser (CLPF-2400 IPG Photonics Inc.). The IDFG output pulses are focused by a reflecting objective onto our device array (≈45 μm effective FWHM spot size). The IDFG pulses arrive at a repetition rate of ≈81 MHz, and at the focal spot, the IDFG pulses can reach energies up to ≈400 pJ. Lastly, in Fig. 1c, we include the simulated field-enhancement spectrum of our nanotriangle emitters.

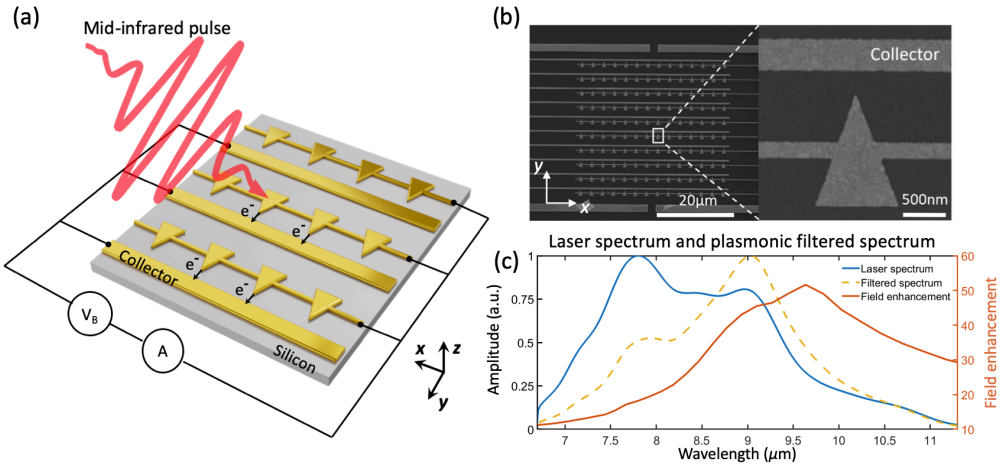

Figure 1: (a) Experimental setup. Mid-infrared laser pulses produce electrical currents from gold nanotriangles. **(b)** Scanning electron microscope (SEM) images of a nanotriangle emitter array. The inset shows the SEM image of an individual nanotriangle and nearby collector. The radius of curvature near the tip of the antenna is ≈10 nm. **(c)** The spectrum of our mid-infrared source, the simulated near-field enhancement of the nanotriangle array, and the resulting local field at the tip of the nanotriangles (excitation spectrum × field enhancement spectrum).

In Fig. 2a, we show emitter current versus IDFG pulse energy. For larger pulse energies, we see that the current closely follows the form I^N where I is the IDFG intensity (proportional to the pulse energy), and $N \approx 2$. The central wavelength of the IDFG corresponds to ≈8 μm, or a photon energy of 0.15 eV (see Fig. 1c). The bandgap in Si is 1.1 eV, and the Schottky barriers formed at the Si and Au/Ti junctions are likely ≈0.6 eV [4]. Therefore, for multiphoton emission, we would expect $N \geq 4$. We attribute the discrepancy in N to strong-field, tunneling emission. It is well-established that in the strong-field regime, the effective emission nonlinearity decreases [1, 2]. Considering the simulated field enhancement of our nanotriangles and measured parameters of our IDFG pulses, we expect to reach the strong-field regime at an incident pulse energy of ≈58 pJ. (Here, the Keldysh parameter, γ, equals one.) Fitting a Fowler-Nordheim emission curve to our data, we find reasonable agreement for pulse energies >58 pJ. Below this $\gamma = 1$ point, we see a clear deviation from the Fowler-Nordheim fit and from the $\approx I^2$ scaling, as our emission departs from the strong-field regime. As a last note regarding Fig. 2a, we should emphasize that we recorded infrared-sensitive currents when illuminating our devices with pulse energies from 10-400 pJ, and for our highest pulse energies, these currents exceeded 6 μA.

In Fig. 2b-d, we include further current measurements from our nanotriangle emitters. Firstly, we note that our devices, with their emitter-silicon-collector structure, resemble metal-semiconductor-metal (MSM) photodiodes. In Fig. 2b, we plot the current versus bias when illuminated by ambient light. The current-bias curve shows the expected behavior for an MSM photodiode. Furthermore, due to the MSM structure, we expect the response of our device array to have a broad electrical bandwidth. In Fig. 2c, we plot the peaks from the radiofrequency (RF) spectrum of the emitter current when illuminated by our IDFG source. The peaks appear at harmonics of the IDFG repetition rate, and we observe up to the 4th harmonic, ≈324 MHz. Lastly, in Fig. 2d, we leverage the high currents and low effective nonlinearity of our emitters to record an interferometric autocorrelation (IAC) of our IDFG pulses. Due to our $\approx I^2$ emission, the measurement closely resembles a conventional IAC using second-harmonic generation. We compare the measured IAC to that expected from transform-limited pulses filtered by the field enhancement spectrum shown in Fig. 1c. The agreement between the measurement and this calculated IAC demonstrates that our IDFG pulses are likely close to transform limited. The transform-limited IDFG pulse duration is 68 fs.

In summary, we have demonstrated strong-field emission currents in metal-silicon-metal photodiodes with an effective second-order nonlinearity. These currents reached >6 μA and responded to pulses with energies down to 10 pJ. These integrated emitter arrays might make attractive detectors for ultrafast, mid-infrared radiation.

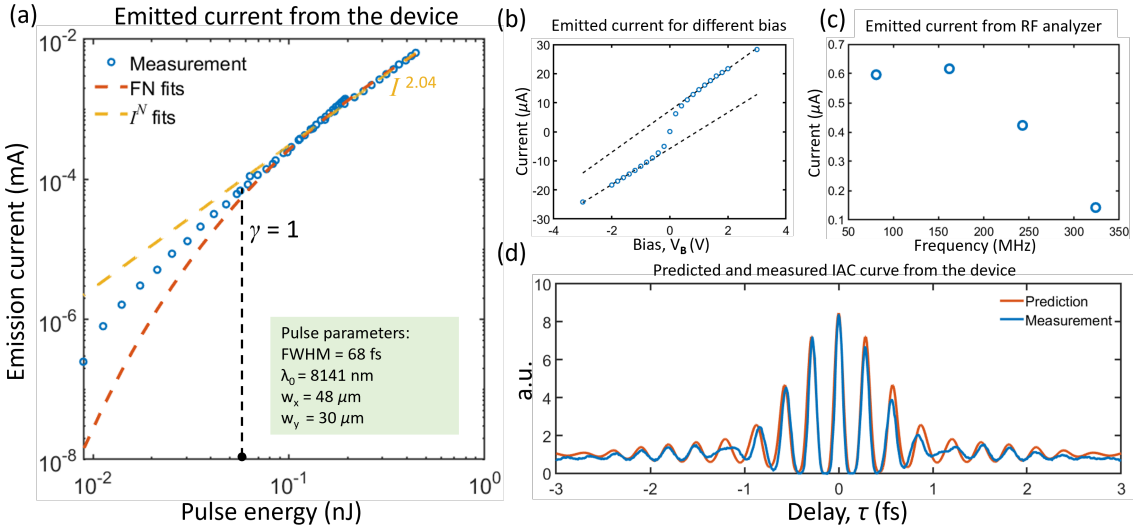

Figure 2: (a) Emission currents from the nanotriangle array (recorded at V_B = 0.4 V). Fowler-Nordheim (FN) and I^N fits are shown. A Keldysh parameter of $\gamma = 1$ is reached at ≈58 pJ. Parameters of the focused IDFG are given in the green box. λ_0 is the center wavelength and w_x and w_y are the Gaussian waist in x and y direction, respectively. **(b)** Measured emitter current for different biases when the device is not illuminated by infrared radiation. (This "infrared dark current" is not included in other measurements.) **(c)** Emitter current peaks from RF analyzer. Points occur at harmonics of the repetition rate of the IDFG. **(d)** Interferometric autocorrelation (IAC) measurements with the emitter current. A predicted IAC, based on the measured pulse parameters and simulated field enhancement, is shown.

References

[1] R. Bormann *et al.*, *Phys. Rev. Lett.*, **105**, 147601 (2010).
[2] W. P. Putnam *et al.*, *Nat. Phys.*, **13**, 335 (2017).
[3] C. Heide *et al.*, *Nat. Photon.*, **14**, 219 (2020).
[4] C. Hu, *Modern Semiconductor Devices for Integrated Circuits* (Pearson, 2009), Chap. 4.